



Short communication

Studies of doped negative valve-regulated lead-acid battery electrodes

K. Micka^{a,*}, M. Calábek^b, P. Bača^b, P. Křivák^b, R. Lábus^b, R. Bilko^b^a J. Heyrovský Institute of Physical Chemistry, ASCR, 182 23 Prague 8, Czech Republic^b Department of Electrotechnology, University of Technology, 602 00 Brno, Czech Republic

ARTICLE INFO

Article history:

Received 6 October 2008

Received in revised form 8 January 2009

Accepted 8 January 2009

Available online 19 January 2009

Keywords:

Lead-acid

Negative electrode

Sulfation suppression

ABSTRACT

Accelerated cycling in the partial state of charge regime showed conclusively that the improvement in cycle life of negative lead accumulator electrodes can be brought about not only by the addition of various sorts of powdered carbon into the active mass but also by the addition of other powdered inert materials like glass fibers, alumina, or titanium dioxide. Steric hindrance of the crystallization of lead sulfate in the electrode pores evidenced by ESEM microphotographs is considered as the main reason for this effect. The added powdered substances were practically without influence on the hydrogen overpotential; and their effect on the active material resistance was also negligible.

© 2009 Elsevier B.V. All rights reserved.

1. Introduction

In our preliminary communication [1], we have discussed the phenomenon of suppressed sulfation of negative lead-acid battery electrodes in the presence of powdered graphite and we came to the conclusion that the electrical conductivity of graphite is not a factor in this case. This reasoning has been supported by our experiments with cells in the flooded system showing that the addition of titanium dioxide produces an effect very similar to the addition of graphite. Since suppression of sulfation is very important for VRLA batteries intended for hybrid electric vehicles and operating in the partial state of charge (PSoC), we considered worthwhile to undertake extensive experiments in hermetic systems using negative electrodes doped with selected powdered materials. Simultaneous measurements of electrode potentials, cell voltage, and gas overpressure in the cell, active mass resistance, and interphase (contact) resistance were carried out to obtain a deeper insight into the studied problem. The influence of the additives on the hydrogen overpotential was checked by special experiments. To be able to make a large number of tedious long-term experiments, an electronic apparatus was built that carried out the accelerated PSoC cycling automatically.

2. Experimental

2.1. Electrodes and cells

We employed pasted negative electrodes of dimensions 55 mm × 20 mm × 2 mm placed between two pasted positives of

dimensions 75 mm × 70 mm × 1 mm (cut out from commercial starting batteries) with 1.8 mm thick AGM separators of the type BG-280GB180 (Hollingsworth&Vose Co.). The lead grids were of the composition Pb Ca 0.2 Sn 0.5%. The initial capacity of the negative electrodes was about 2 Ah. The electrode packs were placed in vented cells filled with sulfuric acid of 1.28 g cm⁻³ density, allowed to stand for an hour, and then subjected to formation by 4 h charging at 0.2 A, 2 h standing on open circuit, and again, in total 72 h charging and 36 h standing. Afterwards, several conditioning cycles were performed: discharging at 0.5 A, charging at 0.5 A for 8 h with voltage limitation to 2.45 V, *i.e.* 2 cycles a day. The test cells (in the vented state) were then subjected to accelerated cycling to determine their cycle life.

It was of interest, in view of the commercial VRLA cells, to arrange more experimental runs by using hermetically closed cells. These were prepared as indicated above except that the excess electrolyte was, after four conditioning cycles in the flooded state, removed, the cells were hermetically closed, discharged to determine their capacity (with a current C_4) and charged with constant current with voltage limitation to 2.45 V as above. Thus, they obtained 105–110% of the original charge.

2.2. Accelerated cycling tests

Accelerated cycling in the PSoC regime was done as follows: Prior to every experimental run, the cells were discharged to 50% capacity measured in the preceding conditioning cycle. During accelerated cycling, both discharging and charging currents were kept constant in the range 1–4 A during the whole cycle life. In the first run, the cells were cycled in this way until their voltage dropped below 1.6 V. Afterwards, the cells were again subjected to several conditioning cycles and a new run was carried out. For com-

* Corresponding author. Tel.: +420 26605 3287; fax: +420 286 582 307.
E-mail address: karel.micka@jh-inst.cas.cz (K. Micka).

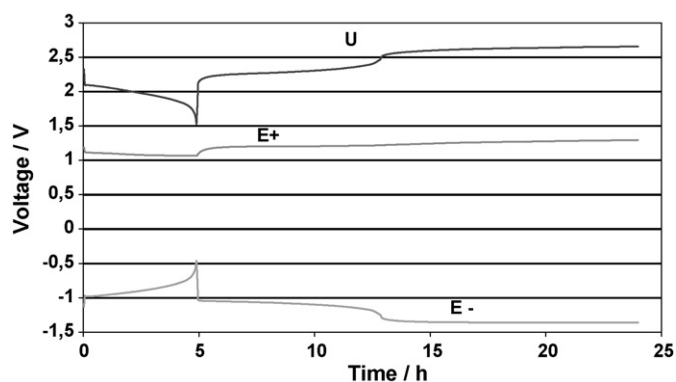


Fig. 1. Potential-time curves for discharging negative electrode with 1% of TiO_2 . U cell voltage, E_+ (+ or $-$) electrode potential vs. $\text{Hg}/\text{Hg}_2\text{SO}_4$.

parison, some runs were done by cycling with a different current (see further text). In some instances, the interphase resistance, R_k , and the active mass resistance, R_m , were measured by our method described earlier [2].

2.3. Measurement of hydrogen overpotential

From the practical point of view, there is a concern whether the additives have an influence on the evolution of hydrogen during charging the electrodes. Therefore, the overvoltage of hydrogen on the negative electrodes was followed in a separate run in vented cells, where the electrode potential was measured against a mercurous sulfate reference. In a conditioning cycle, the cell was discharged at constant current of 0.6 A for about 4 h and charged for 20 h to 150% of the obtained capacity. The potentials of both electrodes, E_+ and E_- , together with the cell voltage, U , were recorded during subsequent discharge. For every admixture, two identical negative electrodes were prepared to obtain two independent results.

3. Results and discussion

3.1. Hydrogen overpotential

The recorded potential–time curves are illustrated in Fig. 1 where the lowest curve corresponding to the negative electrode potential shows the second charge step that was used to evaluate the hydrogen overpotential. The diagrams corresponding to the other negative electrodes investigated were very similar.

The measured data are summarized in Table 1. It can be seen that the scatter of the data is rather small so that the influence of

Table 1
Hydrogen overpotential on doped lead electrodes.

#	Admixture	E_- [V]
1	1% CR 2996	–1.343
2	1% CR 2996	–1.418
3	1% APH 2939	–1.361
4	1% APH 2939	–1.384
5	1% N 134 milled c. black	–1.334
6	1% N 134 milled c. black	–1.385
7	1% nanocarbon	–1.351
8	1% nanocarbon	–1.329
9	1% TiO_2	–1.360
10	1% TiO_2	–1.376
11	White corund 1200	–1.330
12	Corund almatiss 3000	–1.350
13	Without admixture	–1.374
14	Without admixture	–1.375

the admixtures on the hydrogen overpotential is unimportant. The average of the measured data is -1.36 ± 0.02 V.

Here, CR2996 denotes powdered graphite from the firm Maziva (lubricants), Týn/Vlt., Czech Republic (mean particle size $4 \mu\text{m}$), APH 2939 denotes purified flake graphite from Superior Graphite Co., Chicago, IL, USA, N 134 carbon black from S.D. Richardson Co., Acron, OH, USA. Powdered TiO_2 ($1\text{--}3 \mu\text{m}$) was obtained from Lach-Ner Co., Neratovice, Czech Rep., and multiwall carbon nanotubes ($3\text{--}10 \text{nm} \times 1\text{--}3 \text{nm} \times 0.1\text{--}10 \text{nm}$) from Sigma–Aldrich. Corund samples ($2\text{--}3 \mu\text{m}$) were from Carborundum Electric, Benátky, Czech Republic.

It is perhaps interesting to note that when more conditioning cycles were performed during several days the measured hydrogen overpotential dropped slightly, the new average value being 1.26 ± 0.02 V and, after repeating the procedure, it remained practically changeless. Thus, the second discharge step diminished slightly. A possible explanation may be that some impurities were leached out from the positive electrodes and were absorbed by the negative where they lowered the hydrogen overpotential. An effect of the oxygen evolved at the positives seems less probable since vented cells were used.

3.2. Results obtained in the flooded regime

We employed six negative electrodes with the following additives: 2.5% TiO_2 , 1% TiO_2 , 0.5% TiO_2 , 1% and 0.5% graphite CR 2996, and without additive. Six PSoC cycling runs were performed, each ending at 1.6 V of cell voltage. Both the charge and discharge currents were set equal to 1 A for 20 s, standing time was 2 s. As soon as one run was finished, the cells were subjected to four conditioning charge–discharge cycles and another run started. After the fourth run, the electrodes with 0.5% of TiO_2 , 2.5% TiO_2 and 0.5% graphite disintegrated and they had to be removed. The cumulative cycle life of the electrodes under test is illustrated in Fig. 2.

It can be seen that the negative electrode containing 1% TiO_2 showed the best performance exceeding 200,000 cycles. The performance of the electrodes with graphite and without any addition was also quite good (more than 150,000 cycles).

Additional experiments were made with electrodes containing glass fibers. There were three types whose length and diameter were assessed microscopically as follows:

- A: $10\text{--}35 \mu\text{m}/0.6\text{--}1.9 \mu\text{m}$;
- B: $15\text{--}70 \mu\text{m}/1.5\text{--}5 \mu\text{m}$;
- C: $15\text{--}70 \mu\text{m}/2\text{--}15 \mu\text{m}$.

Three cells were assembled with negative electrodes containing 1% of fibers A, 2.5% of fibers A, and 2.5% of B. They were subjected to

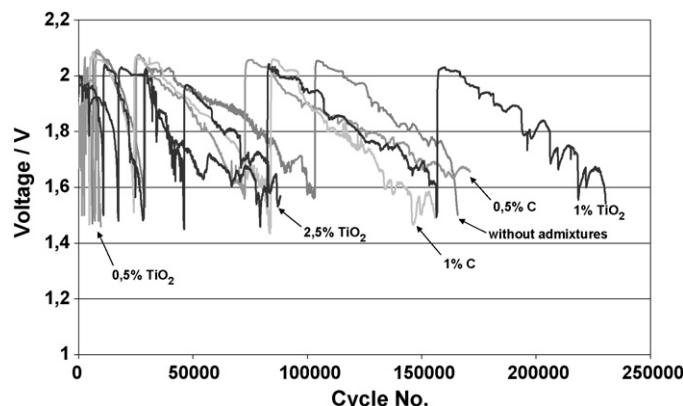


Fig. 2. Cumulative cycle life of electrodes in flooded system.

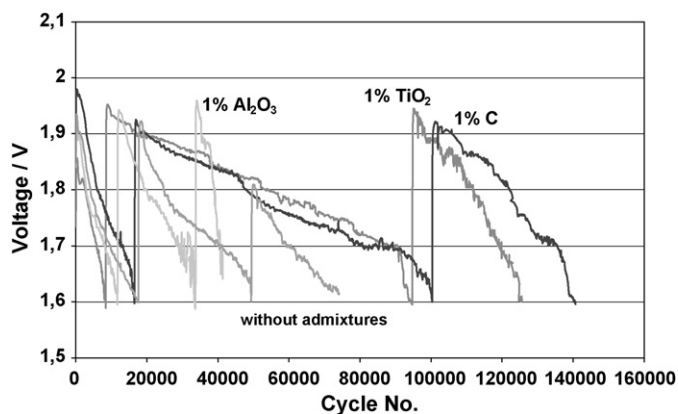


Fig. 3. Cumulative cycle life of electrodes in hermetic system.

accelerated PSoC cycling at a current of 1 A in the flooded regime. Compared to the electrodes mentioned above, the length of the first run (the number of cycles to breakdown) was significantly smaller. The same was true with the subsequent runs, where the electrodes with glass fibers did not surpass 20,000 cycles whereas the electrodes with graphite or titanium dioxide attained 80,000 cycles. Cycling in the hermetic regime is discussed in the next section.

3.3. Results obtained in the hermetic regime

We employed negative electrodes of the following compositions: 1% graphite CR 2996, 1% α - Al_2O_3 , 1% TiO_2 , and without additive. The cycling current was set equal to 2.5 A, the time of charging and discharging was 25 s, and standing 3 s. Thus, the depth of discharge was approximately 0.7% which is slightly higher than the value used by earlier authors (0.52%) [3,4].

The cumulative results obtained from three subsequent runs are shown graphically in Fig. 3.

The cycle life was again highest for the electrode with 1% TiO_2 although slightly shorter than in the preceding case. We assume that this difference is due to the higher depth of discharge used in the PSoC cycling. A similar effect has been observed in experiments with glass fibers described in further text. The results obtained with aluminum oxide are not very hopeful and further experiments would be necessary.

All the carbon samples mentioned in Table 1 were tested under the same experimental conditions as in Fig. 3 and four runs of the PSoC cycling are shown graphically in Fig. 4.

After the cell voltage had dropped to 1.4 V and after several conditioning cycles, another run started. The cycle life of the negative electrodes increased after each run, so the results shown

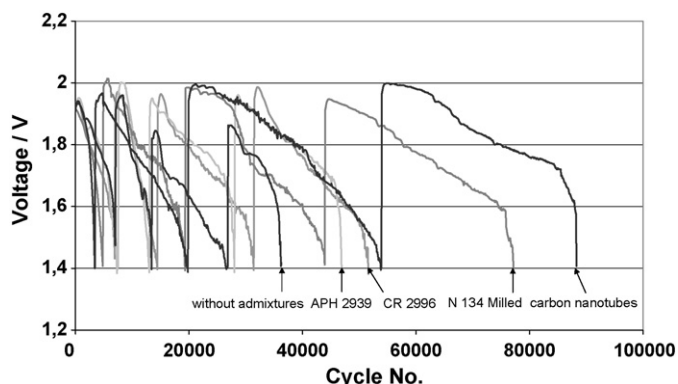


Fig. 4. Cumulative cycle life of carbon-doped electrodes in hermetic system.

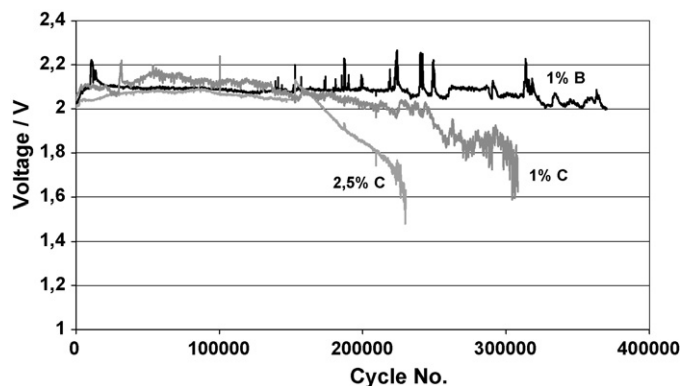


Fig. 5. Cycle life of electrodes doped with glass fibers in hermetic system.

here should be considered as preliminary. While carbon nanotubes showed the best performance, for practical purposes carbon N134 seems to be preferable since it is available in larger quantities.

In preliminary experiments with glass fibers, three test cells were subjected to accelerated PSoC cycling at 1 A. The results were much better than in the flooded regime: the cycle life exceeded 200,000 cycles as can be seen from Fig. 5.

It is probable that a certain compression resulting from the tight electrode assembly is responsible for this improvement. Higher values of the cycling current (3 or 4 A) or deeper cycling (longer duration of the discharge and charge steps), however, seem to cause a significant drop in the cycle life, although only approximate data are available since each experiment was done with a new electrode causing, naturally, some data variations.

3.4. Microstructure of negative electrodes

To find out whether the electrode structure is influenced by the presence of the additives, samples of the electrodes taken in different states of discharge in hermetic cells were investigated by the ESEM method. The electrodes were examined in the charged state. In Fig. 6 is shown a cross section of an electrode without admixtures after 10,000 accelerated cycles, where crystals of lead sulfate are hardly discernible, and in Fig. 7 can be seen the same electrode after 25,000 cycles showing many crystals of lead sulfate.

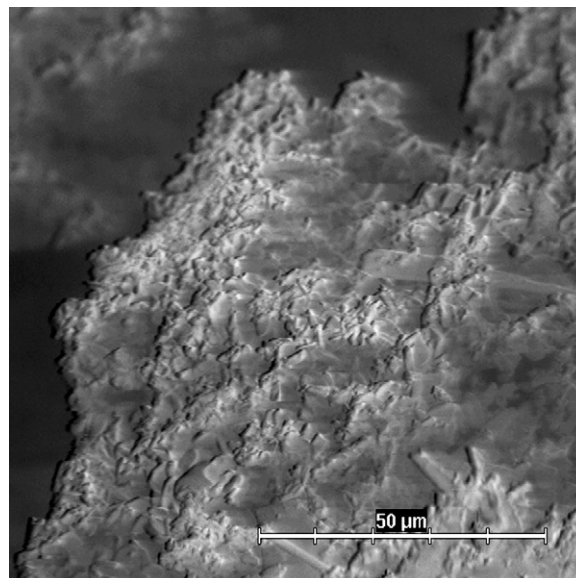


Fig. 6. ESEM microphotograph. Electrode without admixtures after 10,000 cycles.

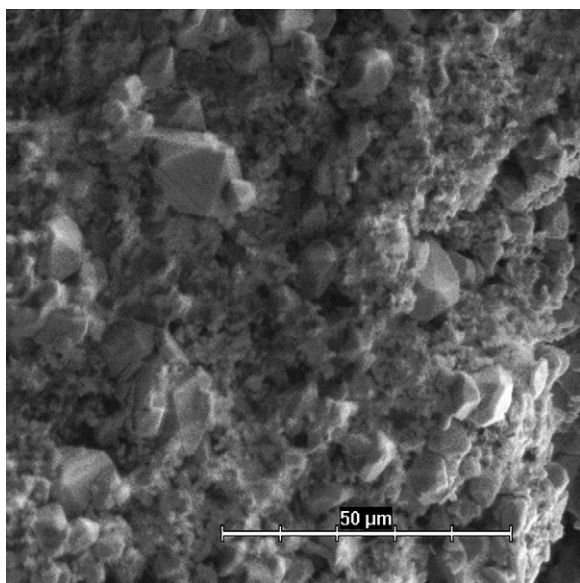


Fig. 7. As preceding but after 25,000 cycles.

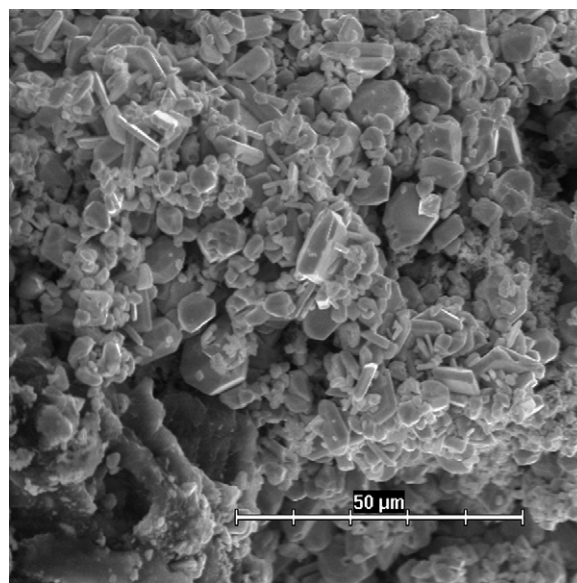


Fig. 9. As preceding but after 42,000 cycles.

Many of these crystals are relatively large ($10\ \mu\text{m}$ or more) so that they could not be converted to lead during charging. An analogous situation can be observed with an electrode doped with titanium dioxide: after 10,000 accelerated cycles (Fig. 8), the crystals of lead sulfate are difficult to recognize, but after 42,000 cycles (Fig. 9) they are apparent, although smaller than in the preceding case (Fig. 7).

And a similar situation was observed with an electrode doped with 1% of graphite. These findings suggest that finely powdered additives in negative lead electrodes bring about a steric hindrance of the growth of lead sulfate crystals and thus they enhance the cycle life during PSoC cycling. The negative electrodes have a relatively small BET surface area of $0.5\text{--}0.8\ \text{m}^2\ \text{g}^{-1}$ [5], hence larger pores, compared to the positives with a BET surface area of about $6.4\ \text{m}^2\ \text{g}^{-1}$ and pores from 0.05 to $2\ \mu\text{m}$ [6,7] that hinder the growth of lead sulfate crystals. Nevertheless, the observed cycle life of the doped negatives was still slightly limited; so it seems that the electrodes under test, being only slightly compressed, suffered some

expansion (a well-known phenomenon with porous lead electrodes) with the result that their pores did grow slightly during prolonged accelerated cycling to accommodate larger crystals. This reasoning is supported by the work [8,9] concerning spirally wound cells where expansion of negative electrodes doped with graphite was obviously prevented by a rigid cylindrical casing, and the cycle life during accelerated cycling in PSoC (under control of the state of charge) approached 200,000 cycles at 2.5% DOD and 60% SoC. Doping with micro-fiberglass was also studied but with unclear effect on the cycle life [8]. Doping with barium sulfate is not very efficient [10].

It is perhaps interesting to note that nonconductive additives (hollow glass microspheres, carboxymethyl cellulose, silica gel, etc.) have been used to improve the performance of positive electrodes [11]. In this case, the primary purpose was to improve the plate porosity.

3.5. Other characteristics

Several characteristics of a test cell measured during the fourth PSoC run, namely the two electrode potentials, the cell voltage, and the gas overpressure, are shown for illustration in a combined diagram (Fig. 10).

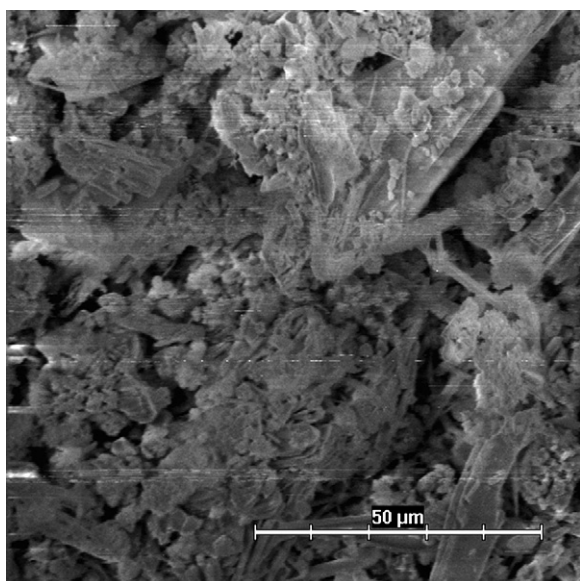


Fig. 8. ESEM microphotograph. Electrode containing 1% of TiO_2 after 10,000 cycles.

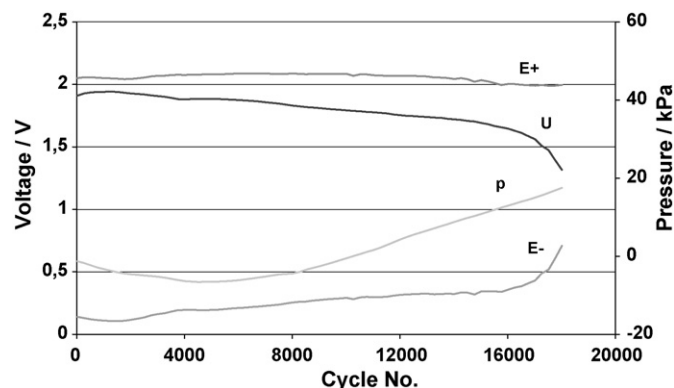


Fig. 10. Voltage, potentials against Cd electrode, and internal pressure during the fourth PSoC run. Electrode containing 1% of graphite APH 2939.

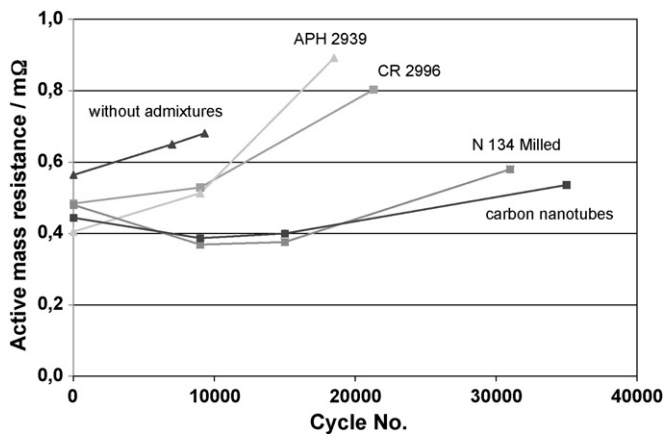


Fig. 11. Dependences of the active mass resistance, R_m , on the cycle number for the fourth PSoC run.

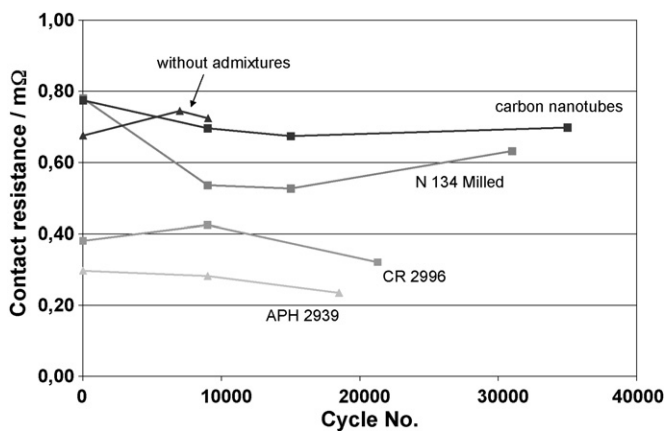


Fig. 12. Dependences of the contact resistance, R_k , on the cycle number for the fourth PSoC run.

The corresponding active mass resistances, R_m , and contact resistances, R_k , in the fourth run are shown graphically in Figs. 11 and 12, respectively.

Since these values are below $1 \text{ m}\Omega$, it may safely be assumed that they are not the cause of the end of the cycle life. Of course, the electrochemical process probably could not affect the whole volume of the active mass owing to the very low depth of discharge, whereas the resistance measurement involved the whole volume of the active mass layer between neighbouring ribs.

Since the contact resistance between the lead grid and the active mass remains practically constant during the whole cycle life (Fig. 12), while the increase in the active mass resistance is relatively small (Fig. 11), it seems that the conspicuous drop in the cell voltage (Fig. 10) during prolonged cycling reflects some passivation of the internal surface of the lead electrode. This passivation would

only affect the surface of the lead particles, hence the electron transfer rate, but neither the resistance between the lead particles nor the contact resistance between the current collector and the lead skeleton. In our previous work [12], it has been shown that negative electrodes operating without mechanical pressure break down soon during deep cycling since the active material volume increases gradually causing an increase of the active mass resistance. The cycling regime used in the present work is relatively very mild and the resistance measurements did not reveal any remarkable change. In our opinion, the reason for the electrode breakdown would be worth of a further study.

4. Conclusions

Accelerated PSoC cycling of laboratory VRLA cells containing doped negative electrodes revealed that the most promising doping agents are titanium dioxide and glass fibers. By comparing the action of different doping agents, it turned out that the most probable mechanism of their action is steric hindrance of the growth of lead sulfate crystals. Titanium dioxide seems preferable in view of its well-defined chemical and granulometric composition, availability, and efficacy.

Acknowledgements

This work was supported by the Advanced Lead-Acid Battery Consortium (Project No. C2.2) and by Research Project CR No. MSM 0021630516. The carbon samples APH 2939 and N 134 were provided by Ian Dyson, CMP Batteries, Ltd. The glass fibers were provided by Tony Ferreira, Hollingsworth&Vose Co., West Groton, MA, USA.

References

- [1] M. Calábek, K. Micka, P. Křivák, P. Bača, J. Power Sources 158 (2006) 864.
- [2] M. Calábek, K. Micka, P. Bača, P. Křivák, V. Šmarda, J. Power Sources 62 (1996) 161.
- [3] M. Shiomi, T. Funato, K. Nakamura, K. Takahashi, M. Tsubota, J. Power Sources 64 (1997) 147.
- [4] L.T. Lan Lam, R.H. Newnham, H. Osgun, F.A. Fleming, J. Power Sources 88 (2000) 92.
- [5] K. Micka, I. Roušar, Electrochim. Acta 21 (1976) 599.
- [6] P. Ekdunge, D. Simonsson, in: K.R. Bullock, D. Pavlov (Eds.), Proceedings of Advances in Lead-Acid Batteries, The Electrochem. Soc., Inc., Pennington, NJ, 1984, p. 252.
- [7] A. Tokunaga, M. Tsubota, K. Yonezu, K. Ando, in: K.R. Bullock, D. Pavlov (Eds.), Proceedings of Advances in Lead-Acid Batteries, The Electrochem. Soc., Inc., Pennington, NJ, 1984, p. 314.
- [8] J. Valenciano, A. Sánchez, F. Trinidad, A.F. Hollenkamp, J. Power Sources 158 (2006) 851.
- [9] M.L. Soria, F. Trinidad, J.M. Lacadena, A. Sánchez, J. Valenciano, J. Power Sources 168 (2007) 12.
- [10] K. Peters, in: K.R. Bullock, T.C. Dayton, D.A.J. Rand, P.T. Moseley, J. Garche, C.D. Parker (Eds.), Valve-Regulated Lead-Acid Batteries, Elsevier, Amsterdam, 2004, p. 135.
- [11] K.R. Bullock, T.C. Dayton, in: D.A.J. Rand, P.T. Moseley, J. Garche, C.D. Parker (Eds.), Valve-Regulated Lead-Acid Batteries, Elsevier, Amsterdam, 2004, p. 109.
- [12] M. Calábek, K. Micka, P. Bača, P. Křivák, J. Power Sources 95 (2001) 97.